Advances in Water Resources 122 (2018) 328–339

Contents lists available at ScienceDirect

Advances in Water Resources

journal homepage: www.elsevier.com/locate/advwatres

# Stochastic water balance dynamics of passive and controlled stormwater basins

Anthony J. Parolari[a,*], Steven Pelrine[a], Mark S. Bartlett[b,c]

[a] Department of Civil, Construction, and Environmental Engineering, Marquette University, Milwaukee, WI 53233, USA
[b] Department of Civil and Environmental Engineering, Duke University, Durham, NC 27708, USA
[c] Department of Civil and Environmental Engineering, Princeton University, Princeton, NJ 08544, USA

ARTICLE INFO

*Keywords:*
Stormwater management
Stochastic hydrology
Real-time control
Urban runoff

ABSTRACT

Urbanization and changing rainfall intensities affect the performance of urban stormwater infrastructure, creating the necessity to design resilient stormwater systems. One proposed method to increase the resilience of stormwater infrastructure is the active control of system flows. To improve the understanding of actively-controlled urban water infrastructure function under variable hydro-climate, we develop a stochastic water balance model for stormwater retention and detention basins with both passive and actively-controlled outflow structures. Under active outflow control, the outflow valve is closed until the water level in the basin reaches a specified maximum at which point the valve opens and the basin empties. Using the stochastic water balance model, we develop analytical expressions for the steady-state probability density functions (PDFs) of water level and valve closure time, as well as the joint PDF of water level and valve closure time. These PDFs then are used to define water level and flow duration curves that provide a probabilistic description of the full range of basin performance. The model accurately predicts the water level PDF estimated from data collected at a retention basin with a passive outflow structure. The model provides a basis for evaluating how changes in the rainfall-runoff process, affected by land use and climate change, will impact the variability of stormwater basin water storage and pollutant removal function. We find that this variability can be managed through the adaptive updating of the active control rule for the outflow structure.

## 1. Introduction

Urbanization and changing precipitation regimes are creating new challenges for urban stormwater management. The impacts of ongoing urbanization on hydrologic response are well known and include increased runoff volume, peak flows, and pollutant concentrations (Leopold, 1968). At the same time, the frequency of extreme intensity precipitation events has increased due to climate change (Kunkel et al., 2013). The interaction of land use and climate change has led to altered rainfall-runoff regimes and hydro-climatic drivers of floods (Yang et al., 2013). Resilient and adaptable infrastructure is needed to manage urban stormwater in this shifting environment.

To offset the impacts of urban development, urban stormwater management systems are designed to mimic pre-development hydrology. However, these designs are often developed in a much simpler hydrologic context that does not reflect operational conditions. Stormwater detention and retention basin designs are commonly based on the runoff volume and peak flow produced during one or a small number of design storms that represent a given return period (NRCS, 1986; Wisconsin Department of Natural Resources, 2007). This “design storm” approach assumes a single operational scenario with an assigned return frequency and thus simplifies the full dynamic range of basin operation that occurs under variable hydro-climatic conditions. Therefore, many existing urban stormwater management systems are not inherently equipped to adapt to land use or climate changes that influence runoff volumes and frequencies. In response to changes in these drivers, functionality may drift over time (Bhaskar et al., 2016; Kerkez et al., 2016). Therefore, new analysis, design, and control approaches are needed to incorporate runoff variability into the understanding of urban water system function.

One opportunity to enhance adaptability and resilience of urban stormwater management systems to long-term change is the active control of system outflows (Mullapudi et al., 2017). The active control of stormwater basin outflows reduces peak outflows and increases pollutant removal efficiency. In response to current rainfall and basin water depth, actively adjusting the outflow gate increased the total suspended solids (TSS) removal efficiency by 44% in one study (Gaborit et al., 2013). Another application achieved greater than 50% reduction in peak flow (Muschalla et al., 2014). While *ad hoc* case studies of ac-

* Corresponding author.
*E-mail addresses:* anthony.parolari@marquette.edu (A.J. Parolari), steven.pelrine@marquette.edu (S. Pelrine), mark.bartlett@duke.edu (M.S. Bartlett).

https://doi.org/10.1016/j.advwatres.2018.10.016
Received 30 March 2018; Received in revised form 16 October 2018; Accepted 16 October 2018
Available online 18 October 2018

tive stormwater control such as these exist, our understanding of how to design active controls to meet hydrologic objectives remains limited (Mullapudi et al., 2017).

A major challenge for water resources management that is especially relevant to operation of active controls is to make effective predictions under large uncertainty from hydro-climate variability. Hydro-climatic variability and active control can be incorporated into models of stormwater infrastructure performance using numerical and analytical approaches. Numerical approaches provide for a continuous simulation of the water balance and hydraulic routing under a time-varying hydro-climate forcing, including several sequential dry and wet weather periods. Analytical methods can be applied using a derived distribution approach in cases where the underlying physical model is sufficiently mathematically tractable. Derived distributions have been used to estimate temporal variability in runoff volume (Chen and Adams, 2007) and pollutant loading (Loganathan and Delleur, 1984) arising from temporal rainfall variability. More recently, Bartlett et al. (2016a; b) used a similar approach to transform spatial variability in rainfall and antecedent soil moisture into spatial variability of runoff generation and spatially-lumped rainfall-runoff curves.

Beyond the derived distribution approach, stochastic differential equations (SDEs) combines the variability of the hydro-climatic forcing with the temporal state dynamics of the infrastructure. In particular, one may pose a corresponding master equation that describes the temporal evolution of the probability density for the SDE state variable. SDEs and the corresponding master equations have been used to model catchment response and streamflow variability (Mejía et al., 2014; Bartlett et al., 2015), variability of stormwater runoff pollutant concentrations (Daly et al., 2014), hydrologic operation of green roofs (Guo, 2016), and the stochastic soil moisture dynamics of biofiltration systems (Daly et al., 2012). These models account for interaction between the external hydro-climatic forcing and the system state and provide clear analytical links between climate, land use, runoff, and function of engineered hydrological systems.

In this paper, we study the interaction between climate variability and active outflow control and its effect on the operation of stormwater basins. Toward this end, we develop a stochastic water balance equation and then analyze the stochastic dynamics of water storage in passive and actively controlled stormwater detention and retention basins. For the stochastic water balance, we derive and solve the analogous master equation for analytical expressions for the steady-state probability density functions (PDFs) of the basin water level and outflow closure time. The water level PDF yields the level and flow duration curves and the ensemble average water balance at the seasonal scale. The outflow closure time PDF provides insight into the actively controlled basin water retention time. Solutions are derived for passive and actively controlled outflow structures for different stage-discharge curves. This probabilistic characterization of stormwater basin function provides a basis for quantifying risk-based metrics, such as the outflow exceedance probability, and adaptive management through active outflow control in terms of climate and basin characteristics.

## 2. Model description

### 2.1. Water balance equation

The water balance for a stormwater basin under active or passive outflow control is conceptualized as a one-dimensional dynamical system with the state variable, $h$, the water depth in the basin. The water balance for a generic basin can be written as,

$$\frac{dV(h,t)}{dt} = Q_i(t) - E_0(t)A_s(h) - Q_s(h,t) - Q_o(h) - L(h,t) \quad (1)$$

where $V(h,t)$ is the water volume in the basin, $Q_i(t)$ is the time-dependent inflow hydrograph from stormwater runoff, $E_0(t)$ is the potential evaporation rate, $A_s(h)$ is the basin surface area, $Q_s(h,t)$ is the state-dependent

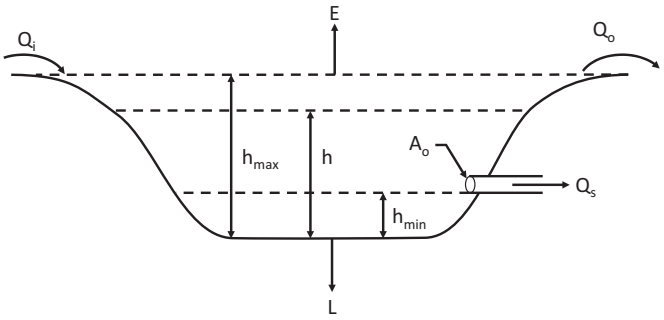


**Fig. 1.** Schematic diagram of the stormwater basin water balance (Eq. (1)): water level depth ($h$), inflow ($Q_i$), overflow ($Q_o$), evaporation ($E$), controlled outflow ($Q_s$) through a structure with area ($A_o$), and exfiltration ($L$). The water level $h$ varies between the invert elevations of the outflow structure ($h_{min}$) and the emergency overflow ($h_{max}$).

structure outflow, $Q_o(h)$ is the emergency overflow, and $L(h, t)$ represents exfiltration to (or infiltration from) the surrounding groundwater (Fig. 1). $Q_s(h,t)$ represents the stage-discharge curve of the outflow structure, which may vary with time in an active control scenario. Both passive and controlled outflows are considered below.

The water balance (1) is simplified for analytical tractability. We assume the basin is rectangular, such that the surface area $A_s$ is constant with depth. We assume evaporation from the water surface and exfiltration are negligible compared to the rates of inflow and outflow. And, finally, we assume there is a minimum water level, $h_{min}$, below which no outflow occurs and a maximum water level, $h_{max}$, above which emergency overflow occurs. The minimum water level corresponds to the invert elevation of the outflow structure. When $h_{min} = 0$, the basin completely empties (i.e., dry pond, detention basin) and when $h_{min} > 0$, the basin retains a permanent pool of water which provides additional pollutant removal (i.e., wet pond, retention basin).

Under the assumptions above, the water balance can be written as a non-linear ordinary differential equation (ODE) for $h$ with a time-varying inflow forcing, $Q_i(t)$, and state-dependent outflow rate, $Q_o(h) + Q_s(h,t)$,

$$A_s \frac{dh}{dt} = Q_i(t) - Q_o(h) - Q_s(h,t). \quad (2)$$

### 2.2. Inflow hydrograph

For urbanized watersheds with a time to peak inflow that is much shorter than the emptying time of the basin, it is reasonable to assume the inflow hydrograph results in an instantaneous jump in the basin water level at the daily time scale, denoted on a normalized basis as $q_i(t) = Q_i(t)/A_s$. Therefore, the inflow from stormwater runoff is modeled as a stochastic jump process and Eq. (2) becomes a stochastic differential equation (SDE) with a non-linear, time-dependent outflow. The inflow $q_i(t)$ is modeled at the daily scale as a marked Poisson arrival process with a constant mean inter-arrival time, $\lambda^{-1}$ (d), and exponentially-distributed runoff volumes with mean depth $\alpha$ (m). These assumptions have been applied in other studies (Chen and Adams, 2007; Daly et al., 2012) and the accuracy of this assumption for the present study is evaluated in Section 3.4 below. Finally, it is assumed that the emergency overflow results in an instantaneous water loss, effectively imposing an upper bound of $h_{max}$ on the basin water level.

For the assumptions outlined above, the distribution of stormwater runoff inflows can be written as (Laio et al., 2001),

$$p_{q_i}(h, q_i) = \frac{1}{\alpha}\exp\left(-\frac{q_i}{\alpha}\right) + \delta(q_i - h_{max} + h)\exp\left(\frac{h_{max} - h}{\alpha}\right) \quad (3)$$

where the exponential distribution of the first term represents inflows without overflow initiation and the Dirac delta function, $\delta(\cdot)$, and expo-

**Table 1**
Stage-discharge relations normalized by stormwater basin surface area and corresponding water level trajectories $h(t)$ for several common outflow structures. Stage-discharge relations are written in a general form as $\rho(h) = kh^b$ and the parameters are $C_d$, discharge coefficient, $g$, gravitational constant (m/s$^2$), $A_s$, basin surface area (m$^2$), $A_o$, orifice area (m$^2$), $L$, weir length (m), $\theta$, angle of weir notch (°), and $Q$, constant discharge rate (m$^3$/s). In the final column, the water level trajectory $h(t)$ is reported for the initial condition $h(0) = h_0$.

| Outflow type | Stage-discharge coefficient, $k$ [m d$^{-1}$] | Stage-discharge exponent, $b$ | Basin inter-storm water level trajectory, $h(t)$ |
|---|---|---|---|
| Constant | $\frac{Q}{A_s}$ | 0 | $h(t) = -kt + h_o$ |
| Orifice | $\frac{C_d A_o \sqrt{2g}}{A_s}$ | 1/2 | $h(t) = \frac{1}{4}k^2t^2 - k\sqrt{h_o}t + h_o$ |
| Sharp-Crested Rectangular Weir | $\frac{2}{3}\frac{C_d L \sqrt{2g}}{A_s}$ | 3/2 | $h(t) = 4(kt + \frac{2}{\sqrt{h_o}})^{-2}$ |
| Broad-Crested Weir | $1.71\frac{C_d L}{A_s}$ | 3/2 | $h(t) = 4(kt + \frac{2}{\sqrt{h_o}})^{-2}$ |
| V-notched Weir | $4.28\frac{C_d \sqrt{2g}\tan(\frac{\theta}{2})}{A_s}$ | 5/2 | $h(t) = \left(\frac{3}{2}kt + h_o^{-3/2}\right)^{-2/3}$ |

nential function represent the discrete probability of $q_i > h_{max} - h$, i.e., an inflow that produces an overflow event.

### 2.3. Outflow hydrograph: Passive and active control

Active control of stormwater basin outflows may be designed to meet a wide range of operational water quantity and quality criteria. These criteria include limiting outflow rates to minimize increases above pre-development conditions or enhancing the settling of suspended pollutants through increased detention time. A common approach that offers a relatively simple starting point is "on/off" i.e., bang-bang control (Jacopin et al., 2001; Muschalla et al., 2014). The on/off control specifies a maximum water level set-point, denoted $h_s$, that triggers the outflow structure to open to its maximum area. Once the basin empties to the level $h_{min}$, the outflow structure is closed until the set-point is reached again.

Both passive and actively controlled outflows can be modeled in the water balance Eq. (2). For both cases, we specify a stage-discharge relation with the general form

$$\rho(h) = \frac{Q_s(h)}{A_s} = \begin{cases} 0 & h = h_{min} \\ kh^b & h > h_{min} \end{cases}, \tag{4}$$

for which the parameters $k$ [cm d$^{-1}$] and $b$ [-] for passive outflow structures, such as orifices and weirs, are summarized in Table 1. Passive outflow structures are fully specified by Eq. (4), whereas actively-controlled outflow structures require specification of the on/off rule which is introduced in the solution to the water balance equation derived in Section 3.4.

### 2.4. Case study

The model performance was evaluated for the water level in a stormwater retention basin controlled by a passive outflow located in Ann Arbor, MI (Kerkez et al., 2016; Mullapudi et al., 2017). The basin has a maximum surface area of 8400 m$^2$ at a water depth of 248 cm and a minimum surface area of approximately 3900 m$^2$ at the invert elevation of the outflow structure. The outflow structure consists of two circular, 2-m diameter pipes. The pond water level was recorded at 5-min intervals over a 3-month period between August 1 and October 20, 2016. The depth and arrival time of individual runoff events were extracted from the water level time-series to estimate the average inflow depth and average inflow frequency parameters $\alpha$ and $\lambda$. The assumption of exponentially distributed inflow depths and inflow arrival times was verified using the 2016 water level data and daily rainfall data obtained from the city of Ann Arbor (http://www3.a2gov.org/RainGauges/), spanning the years 2010–2018. The outflow stage-discharge relation was estimated from the observed water level recession between events.

### 2.5. Model simulations

Numerical and analytical results are presented below. The analytical model solutions are developed in Section 3.1 through Section 3.4, which are evaluated directly for a given set of parameters. To verify the analytical model solutions, numerical simulations of the water balance were implemented in MATLAB using a forward Euler explicit time-stepping scheme. Runoff inflows and inter-event times were sampled from the corresponding distributions and a 30-year time-series of stormwater runoff inflow events was generated.

## 3. Results

The following section describes the deterministic and stochastic analysis of Eq. (2). In Section 3.1, the deterministic dynamics of the basin drainage process are presented for each of the outflow stage-discharge relationships listed in Table 1. In Sections 3.2 and 3.4, we examine the stochastic balance SDE, present the analogous master equation for steady state conditions, and solve the master equation for the probability density function of water level, $p_h(h)$, under passive and active control scenarios, respectively. In Section 3.3, the performance of the model for a passive control scenario is demonstrated. Finally, in Section 3.5, summary statistics relevant to hydrologic function and design, including the level and flow duration curves and the PDF of the valve closure time, are analyzed and discussed.

### 3.1. Deterministic solution for a single drainage event

For a single drainage event, $q_i(t) = 0$. The resulting ODE $dh/dt = -\rho(h)$ was solved with initial condition $h(t = 0) = h_0$ and $h_{min} = 0$ for each of the $\rho(h)$ expressions in Table 1. The resulting trajectories $h(t)$ are summarized in Table 1 and Fig. 2. Note that for constant and orifice outflow stage-discharge relations (or any power law with $0 \le b < 1$), $h$ reaches $h_{min}$ in finite time. For this case, the inter-storm water level trajectory is only valid for $0 < t < t_f$, where $t_f$ satisfies $h(t_f) = h_{min}$. These dynamics imply the basin spends a finite, non-zero fraction of time in an empty state, a point which will become clear in the probabilistic analysis below.

### 3.2. Steady-state probability distribution of water level: passive outflow

For the water balance in Eq. (2) forced by the runoff inflow distribution (3), the general solution for the steady-state PDF of water level is derived from a master equation for the Cumulative Distribution Function (CDF) in steady state. In steady state, this master equation may be derived as a balance of the upcrossing and downcrossing rate of any water level, $h$ (Brill, 2008; Bartlett et al., 2015), i.e.,

$$\rho(h)p_h(h) = \lambda \int_{u=0}^{h} \exp\left(-\frac{h-u}{\alpha}\right) p_h(u)du \tag{5}$$

**Table 2**
Steady-state water level probability density functions for different outflow stage-discharge relations. For brevity, the normalization constants, $N$, are not reported here, but can be found by imposing the normalizing condition, $P(h_{max}) = 1$.

| Outflow type | Steady-state water level PDF, $p_h(h)$ | Atom of probability, $P_0$ |
|---|---|---|
| Constant | $\delta(h)P_0 + \frac{\lambda P_0}{k}\exp\left(-\frac{h}{\alpha}+\frac{\lambda}{k}h\right)$ | $\frac{\alpha\lambda - k}{\alpha\lambda[1+\exp\left((-\frac{1}{\alpha}+\frac{\lambda}{k})h_{max}\right)]-k}$ |
| Orifice | $\delta(h)P_0 + \frac{\lambda P_0}{k}h^{-0.5}\exp\left(-\frac{h}{\alpha}+2\frac{\lambda}{k}h^{0.5}\right)$ | $\frac{k}{k-\sqrt{\alpha\pi}\lambda\exp(\frac{\alpha\lambda^2}{k^2})[1-\mathrm{erf}(\frac{\alpha\lambda-k\sqrt{h_{max}}}{\sqrt{\alpha}\,h_{max}})]}$ |
| Rectangular Weir | $N\frac{h^{-1.5}}{k}\exp(-\frac{h}{\alpha}-2\frac{\lambda}{k}h^{-0.5})$ | 0 |
| V-notched Weir | $N\frac{h^{-2.5}}{k}\exp(-\frac{h}{\alpha}-\frac{2}{3}\frac{\lambda}{k}h^{-1.5})$ | 0 |

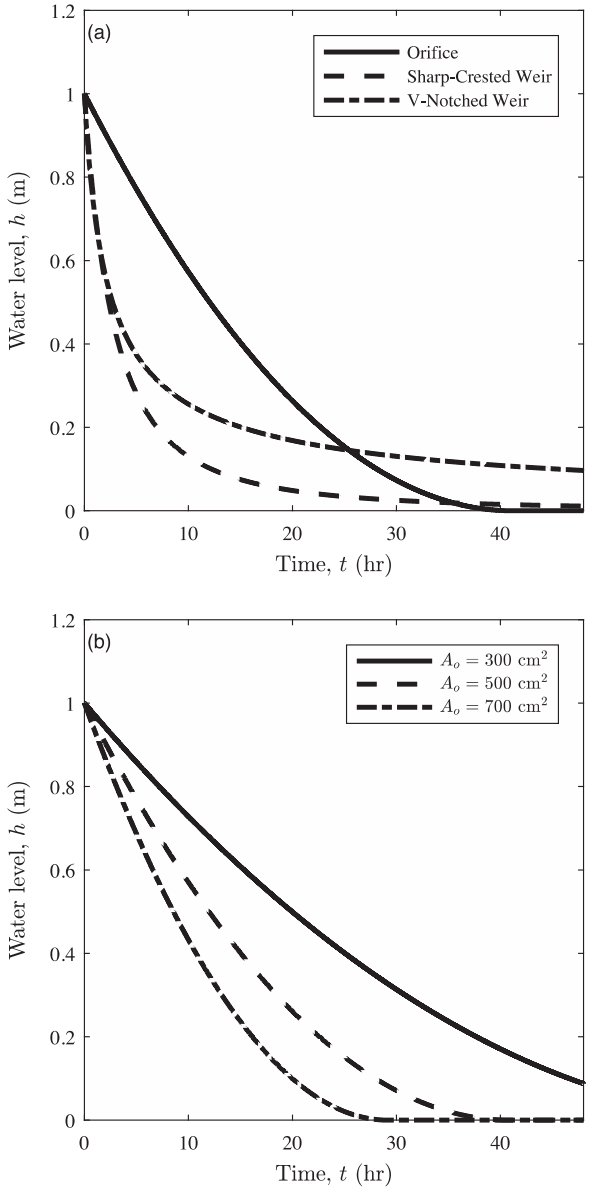


**Fig. 2.** Time trajectories of $h(t)$ for different outflow structures (a) and different values of the orifice area, $A_o$ (m$^2$) (b). Other parameters are: $h_i = 1$ m, $h_{min} = 0$ m, $A_s = 10,\ 000$ m$^2$, $L = 0.1$ m, $C_d = 0.61$ (orifice), $C_d = 3.33$ (sharp-crested weir), $C_d = 0.62$ (V-notch weir), and $\theta = 22.5^\circ$. In (a), $A_o = 500$ cm$^2$.

where $p_h(h) = f(h) + \delta(h)P_0$ is the steady-state water level PDF, $f(h)$ is the continuous part of the PDF, $P_0$ is an atom of probability at $h = 0$, $h_{min}$ is set equal to 0 for brevity, and $u$ is a dummy integration variable. $P_0$ arises in cases where the water level reaches 0 in finite time. In Eq. (5), the LHS is the downcrossing rate at level $h$ due to outflow and the RHS is the upcrossing rate, accounting for water level jumps due to runoff inflow. By taking the derivative of both sides of Eq. (5) with respect to $h$, one retrieves the master equation for the steady state dynamics of the PDF, $p_h(h)$.

The solution of Eq. (5) is (Brill, 2008; Botter et al., 2009),

$$p_h(h) = \frac{N}{\lambda}\delta(h)\Theta(1-b) + \frac{N}{\rho(h)}\exp\left[-\frac{h}{\alpha} + \lambda\int_0^h \frac{du}{\rho(u)}\right] \tag{6}$$

where the atom of probability at $h = 0$ is $P_0 = \frac{N}{\lambda}\Theta(1-b)$. Note that for $0 \le b \le 1$, $N = \lambda P_0$, which is equivalent to the steady-state probability that an inflow event occurs when $h = 0$. In Eq. (6), $N$ or $P_0$ can be found by imposing a total probability equal to 1, $P(h_{max}) = \int_0^{h_{max}} p_h(h)dh = 1$.

Eq. (6) is the basis for the solution derived from the general stage-discharge curve, $\rho(h)$, of Eq. (4), i.e.,

$$p_h(h) = \frac{N}{\lambda}\delta(h)\Theta(1-b) + \frac{N}{kh^b}\exp\left(-\frac{h}{\alpha} + \frac{\lambda}{k(1-b)}h^{1-b}\right) \tag{7}$$

In turn, the general solution of Eq. (7) is the basis for the specific solutions summarized in Table 2, which are based on the parameters $b$ and $k$ for the different stage-discharge curves of Table 1.

Example steady-state water level PDFs for a passive orifice discharge are illustrated in Fig. 3. Numerical simulations demonstrate that the analytical solution is accurate. The mode of the water level PDF is equal to zero for large values of $A_0$ (Fig. 3a) and increases to positive values as the outlet structure cross-sectional area decreases. The shape of the water level PDF is also sensitivity to the runoff inflow distribution as the mode increases with increasing runoff frequency $\lambda$ (Fig. 3b). That is, climate and watershed characteristics that generate more frequent, less intense runoff are associated with more stormwater basin storage. Therefore, changes in the basin design parameters (e.g., $A_0$) or watershed or climate characteristics (e.g., $\lambda$) can change the most likely basin state from empty (i.e., the mode of $h$ is zero) to partially full (i.e., the mode of $h$ is greater than zero).

### 3.3. Model performance for passive outflow

Visual inspection of the water level data confirms that stormwater runoff inflow events occur much more rapidly than outflow (Fig. 4a), justifying the assumption that inflows events can be treated as an instantaneous, random jump forcing at the time-scale of the basin outflow process. The estimated parameters for the inflow model were $\alpha = 17.2$ cm and $\lambda^{-1} = 3.6$ d, respectively. The distributions of extracted storm depths and inter-storm durations are well-approximated by the exponential distribution (Fig. 4b). From the long-term rainfall data, we

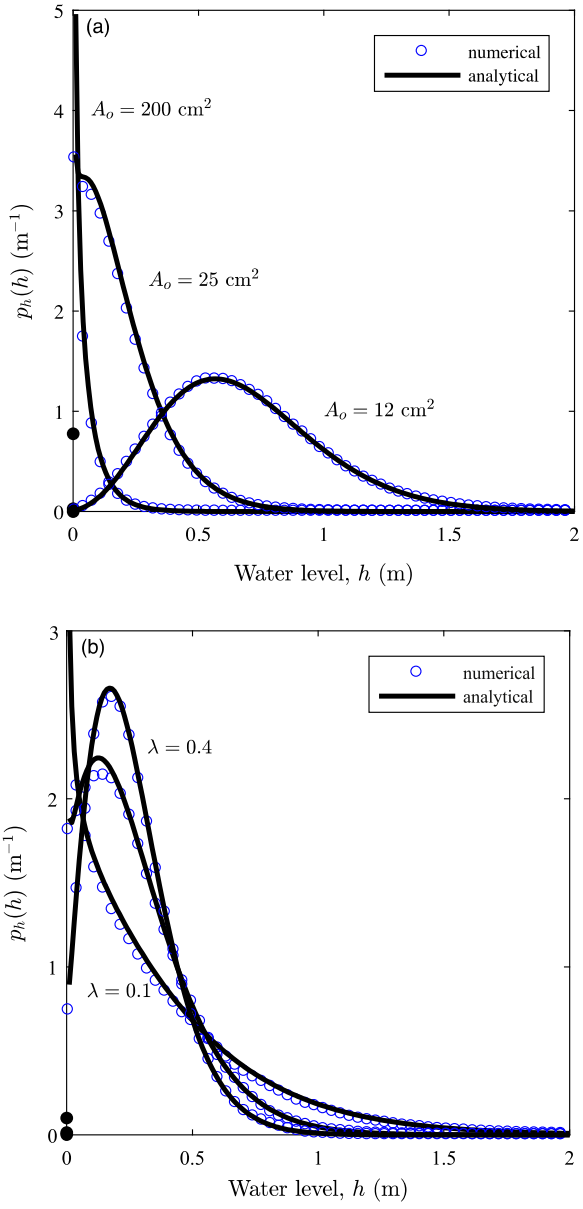


**Fig. 3.** Example water level probability density functions (PDFs) for a passive orifice outflow for (a) several values of $A_o$ and (b) several values of $\lambda$. Other parameters are $h_{min} = 0$, $h_{max} = 2$ m, $\lambda = 0.3$ d$^{-1}$, $\alpha = 7.5$ cm, $C_d = 0.6$, and $A_s = 10,000$ m$^2$. In (b), $A_0 = 20$ cm$^2$ and $\alpha$ is varied such that the total inflow runoff volume is equal. The open circles correspond to the numerical solution, the black lines to the analytical continuous part of the PDF, and the black dots to the analytical atom of probability at $h = 0$.

estimated an average inter-storm duration of 3.0 d and an average daily rainfall depth of 6.8 mm. The distributions of daily rainfall depth and inter-storm duration are also well-approximated by the exponential distribution (Fig. 4c), further supporting our assumption. Note, however, that this assumption may fail for time-series that span seasonal or inter-annual rainfall variability (Porporato et al., 2006).

The outflow stage-discharge relation was estimated from the data (Fig. 5). The outflow process follows two regimes. For water levels greater than 40 cm, the stage-discharge relation follows $\rho(h) \sim h^2$ and for water levels less than 40 cm, $\rho(h) \sim h^3$. The basin water level exceeded 40 cm during one inflow event and for less than 1% of the time period. Further, the estimated outflow rate at high water levels exceeds 100 cm/day. Therefore, at the daily time-scale, we assume that the basin has a maximum water level $h_{max} = 40$ cm and $\rho(h) \sim h^3$. The exponent $b = 3$ is consistent with typical stage-discharge curves for open channel flow in partially full circular cross sections.

For the estimated stage-discharge curve of $\rho(h) = kh^3$, the steady-state water level PDF is,

$$p_h(h) = \frac{N}{k} h^{-3} \exp\left(-\frac{h}{\alpha} - \frac{\lambda}{2k} h^{-2}\right). \tag{8}$$

The outflow coefficient $k$ was estimated by the method of moments and estimated to be $k = 0.026$ cm/d. The modeled and observed CDFs compare favorably for cumulative probabilities greater than 0.01 (Fig. 6).

### 3.4. Steady-state probability distribution of water level: On/Off outflow control

Under active on/off control driven by a single water level set-point, the basin water level dynamics can be in one of two regimes at any given time. In the first regime, the outflow structure is fully closed and the water level increases by successive inflow jumps generated by the watershed rainfall-runoff process. In the second regime, the outflow structure is fully open. When the structure is open, the water level increases by successive inflow jumps and decreases according to the stage-discharge curve between inflow events. Switching between these two regimes is triggered when the water level exceeds the outflow open set-point, $h_s$, (outflow opens) and when the water level reaches $h_{min}$ (outflow closes). For constant and orifice outflow stage-discharge curves, $h$ reaches $h_{min}$ in finite time, whereas for other structures a positive set-point for valve closure must be specified because, in theory, the basin never fully empties. Example water level trajectories for a passive and controlled orifice outflow are compared in Fig. 7.

The steady-state water level PDF for the two-regime system can be written as a weighted sum of the PDF for each regime,

$$p_h(h) = C_1 p_{h_1}(h) + (1 - C_1) p_{h_2}(h) \tag{9}$$

where $C_1$ is the ensemble average fraction of time spent in regime 1 (filling, outflow closed) and $1 - C_1$ is the ensemble average fraction of time spent in regime 2 (emptying, outflow open). The steady-state PDFs $p_{h_1}(h)$ and $p_{h_2}(h)$ and the coefficient $C_1$ can be obtained by evaluating each regime separately.

For the filling regime, we may pose a master equation for the CDF in terms of downcrossing and upcrossing rates. Downcrossing only occurs at level $h = h_{min}$ when the system switches from the emptying to the filling state (i.e., when the outflow closes) and sample-paths are composed of only upcrossings. Therefore, the steady-state balance of downcrossings and upcrossings during the filling process can be written as (Brill, 2008),

$$C_D = \lambda \int_{u=0}^{h} \exp\left[-\frac{h-u}{\alpha}\right] p_{h_1}(u) du \tag{10}$$

where $0 < h \le h_s$, $C_D$ is the average downcrossing rate at which the emptying regime enters the filling regime (i.e., the average rate at which the outflow structure closes), $h_{min} = 0$, and the RHS term accounts for upcrossings due to runoff inflow. Eq. (10) can be solved to obtain the continuous part of the PDF, $f_{h_1}(h) = \frac{C_D}{\alpha\lambda} = \frac{P_0}{\alpha}$, where it is noted that steady-state requires that $C_D = \lambda P_0$, i.e., the rate of downcrossing equals the rate of leaving the level $h = 0$. Finally, applying the normalization condition yields,

$$p_{h_1}(h) = \frac{1}{\alpha + h_s} + \delta(h) \frac{\alpha}{\alpha + h_s} \tag{11}$$

which states that when the outflow is closed, the water level PDF is a mixed distribution with a continuous uniform PDF, i.e., $f_{h_1}(h) = \frac{1}{\alpha + h_s}$, and an atom of probability of $P_0 = \frac{\alpha}{\alpha + h_s}$ at $h = 0$. The distribution only

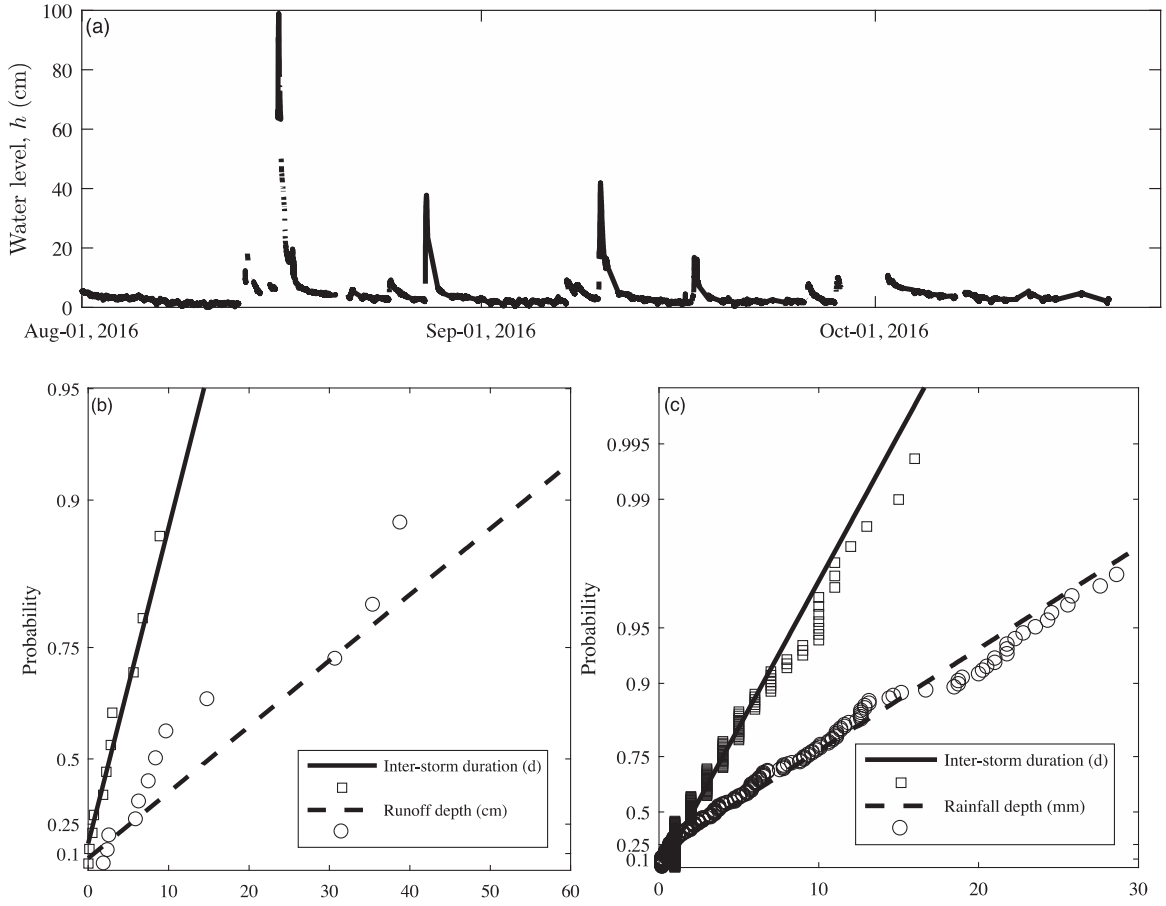


**Fig. 4.** Retention basin water level and rainfall data analysis for Ann Arbor, MI: (a) Observed water level dynamics, (b) comparison of extracted storm depths (circles, dashed line) and inter-storm durations (squares, solid line) to the exponential distribution, and (c) comparison of daily rainfall depths (circles, dashed line) and inter-storms durations (squares, solid line) to the exponential distribution.

depends on the average runoff depth and the on/off set-point, $\alpha$ and $h_s$, respectively.

Likewise for the emptying regime, the steady-state master equation based on the CDF may be derived in terms of a balance of upcrossings and downcrossings, i.e.,

$$\rho(h)p_{h_2}(h) = C_U + \lambda \int_{u=0}^{h} \exp\left[-\frac{h-u}{\alpha}\right] p_{h_2}(u)du \tag{12}$$

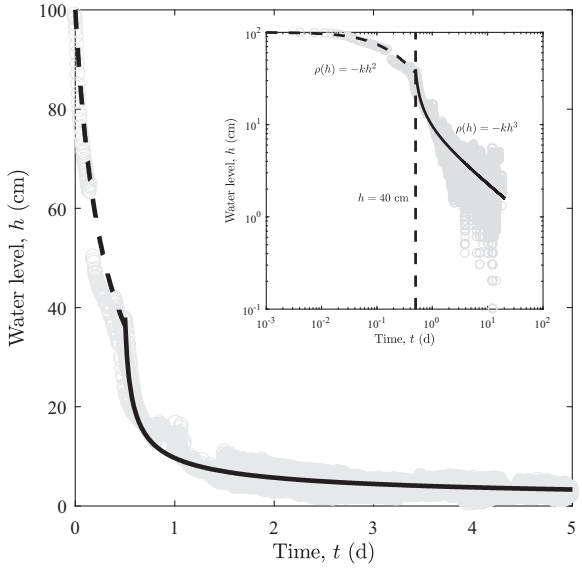


**Fig. 5.** The observed water level as a function of time for the retention basin in Ann Arbor, MI. The dashed line corresponds to $\rho(h) \sim h^2$ and the solid line corresponds to $\rho(h) \sim h^3$. The inset shows the same data plotted in log-log space.

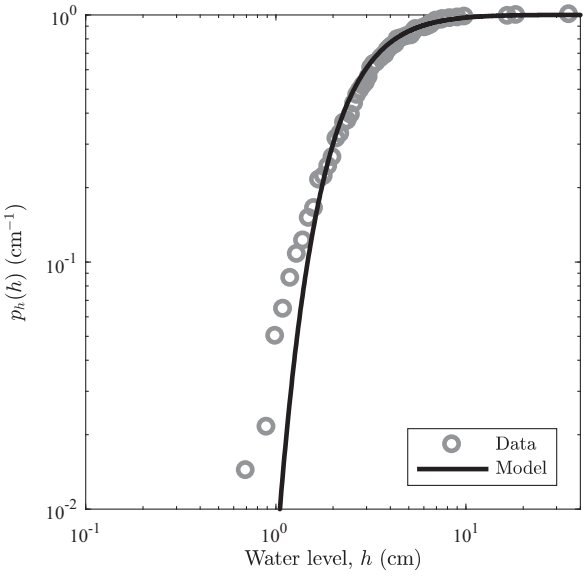


**Fig. 6.** Comparison of the observed (open circles) and modeled (black line) water level cumulative distribution functions (CDFs) for the retention basin in Ann Arbor, MI. The modeled steady-state PDF is given by Eq. (8) in the text. The parameters are $k = 0.026$ cm/d, $b = 3$, $\alpha = 17.2$ cm, and $\lambda^{-1} = 3.6$ d.

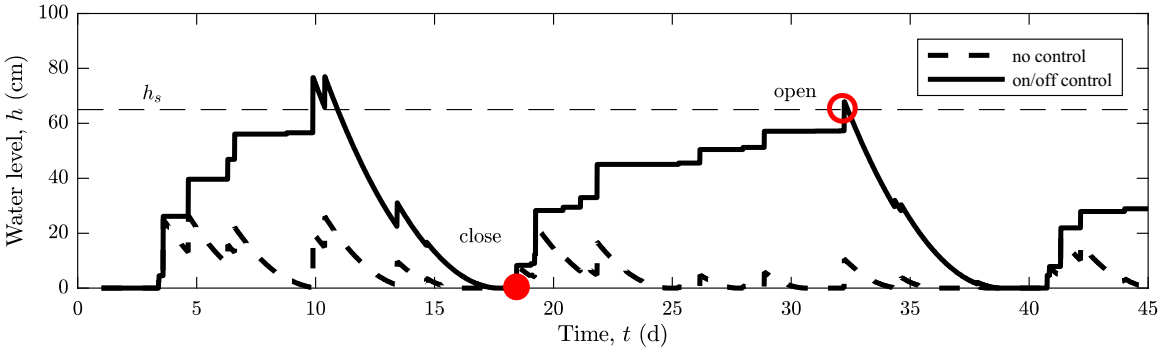


**Fig. 7.** Example trajectories of the stormwater basin water level for passive (gray line) and controlled (black line) outflows. $h_s = 0.65$ m and all other parameters are the same as Fig. 3. The open and closed circles denote the time of valve opening and closing for one cycle.

where $C_U$ is the average upcrossing rate at which the filling regime enters the emptying regime (i.e., the average rate at which $h_s$ is crossed and the outflow structure opens) and the second term on the RHS is the upcrossing rate due to runoff inflow. The LHS of Eq. (12) is the downcrossing rate due to outflow. Eq. (12) can be solved to obtain,

$$p_{h_2}(h) = \frac{C_U}{\rho(h)} \exp\left[-F(h)\right]\left\{1 + \frac{1}{\alpha}\int_{u=0}^{h_s+(h-h_s)\Theta(h_s-h)} \exp\left[F(u)\right]du\right\} \tag{13}$$

where $F(u) = \int_0^u (\frac{1}{\alpha} - \frac{\lambda}{\rho(y)})dy$, $\Theta(\cdot)$ is the Heaviside step function, and the rate $C_U$ is the normalization constant of the PDF such that $\int_0^{h_{max}} p_{h_2}(h)dh = 1$ (see Appendix A). The solution of (13) for the general stage-discharge relation $\rho(h)$ is,

$$p_{h_2}(h) = \frac{C_U}{kh^b} \exp\left[-\frac{h}{\alpha} + \frac{\lambda}{k(1-b)}h^{1-b}\right] \left\{1 + \frac{1}{\alpha}\int_{u=0}^{h_s+(h-h_s)\Theta(h_s-h)} \exp\left[\frac{u}{\alpha} - \frac{\lambda}{k(1-b)}u^{1-b}\right]du\right\}. \tag{14}$$

Finally, the weight $C_1$ can be obtained by noting that, at steady-state, the rate out of the emptying regime (into the filling regime) must be equal to the rate out of the filling regime (into the emptying regime). Therefore, $C_1 C_D = (1 - C_1)C_U$ and,

$$C_1 = \frac{C_U}{C_D + C_U}. \tag{15}$$

The full PDF $p_h(h)$ for an active outflow control is given by Eq. (9), which is based on the functions given by Eqs. (11), (14), and (15). Numerical and analytical solutions for the actively controlled water level PDF are shown in Fig. 8a and the actively controlled water level PDF is compared to the passive water level PDF in Fig. 8b.

### 3.5. Comparing basin performance metrics under passive and active control

In this section, several basin performance metrics are derived from the previously developed PDFs and compared for passive and actively controlled outflows. Probabilistic performance metrics include the level duration curve (LDC), flow duration curve (FDC), the PDF of the valve closure time, and the joint PDF of the water level and the valve closure time. Aggregate performance metrics include the ensemble average water level and outflow water balance.

#### 3.5.1. Level and flow duration curves

The steady-state water level PDF and stage-discharge curve can be used to construct the LDC and FDC. The LDC is the complement of the water level CDF, $L(h) = 1 - P_h(h) = 1 - \int_0^h p_h(h)dh$. The FDC is also the complement of a CDF, but depends on the outflow status in addition to the basin water level. The FDC can be written as,

$$F(q) = \left[1 - P_q(q)\right]\left(1 - C_1\right) = \left[1 - \int_0^q p_q(q)dq\right]\left(1 - C_1\right) \tag{16}$$

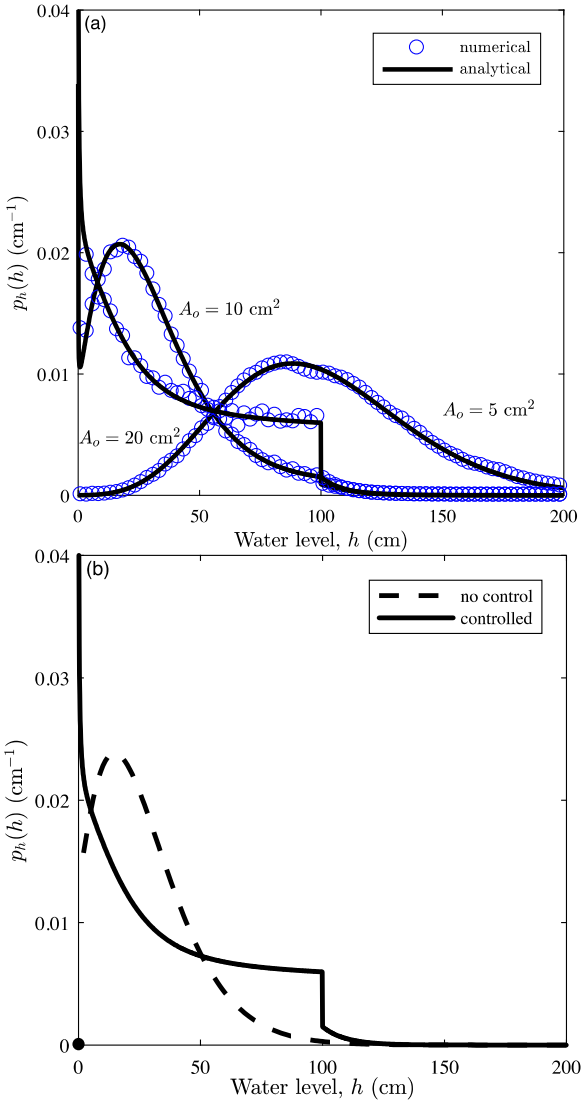


**Fig. 8.** (a) Probability density functions (PDFs) for controlled orifice outflows with several values of $A_o$. (b) Comparison of passive and controlled basins for $A_o = 20$ cm$^2$. $h_s = 1$ m and all other parameters are the same as Fig. 3.

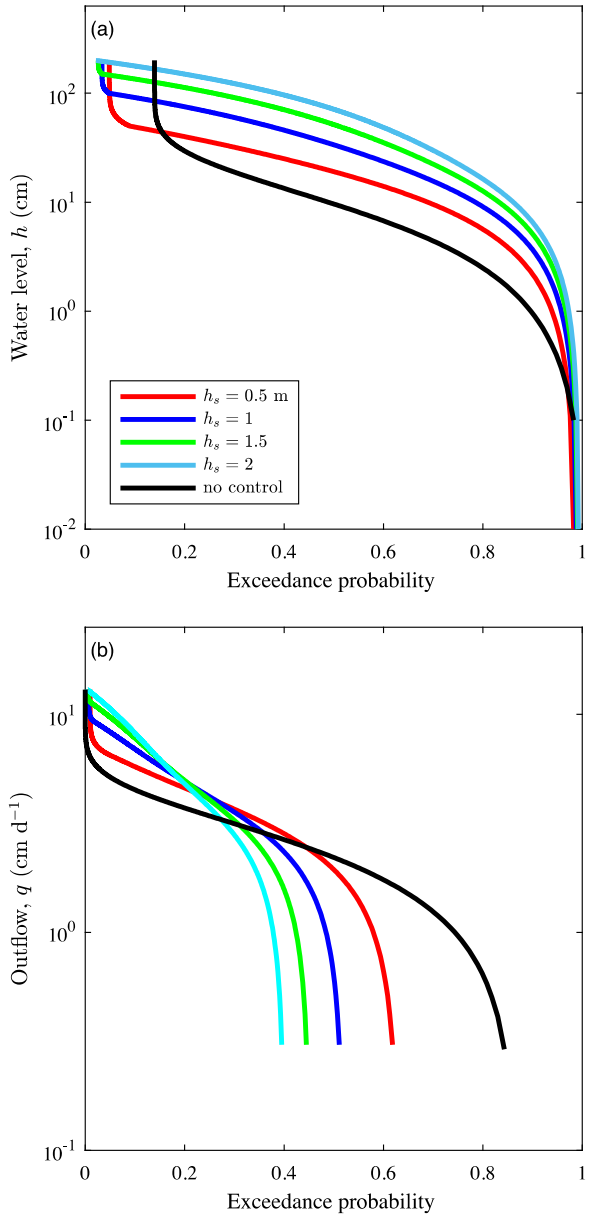


**Fig. 9.** Level duration (top) and flow duration (bottom) curves for passive outflow and actively-controlled outflow with several values of the outflow on/off setpoint. All parameters are the same as those in Fig. 3.

where $p_q(q)$ is the PDF of the outflow rate and $1\text{-}C_1$ is the fraction of time the outflow is open with $q > 0$. The outflow PDF can be obtained as a derived distribution of the water level PDF, $p_q(q) = p_h[(\frac{q}{k})^{\frac{1}{b}}] \cdot |kb(\frac{q}{k})^{b-\frac{1}{b}}|^{-1}$, based on a change of variables following Eq. (4).

Example LDCs and FDCs are plotted in Fig. 9 for an orifice outflow with passive and active control at several on/off setpoints. Compared to passive outflow (no control), active control increases the LDC and, therefore, the water level at most return frequencies. Active control modifies the FDC in two ways. First, positive flows are restricted to the fraction of time, $C_1$, when the basin is in the emptying regime. Secondly, the distribution of flows is modified such that higher flows are more frequent with active control than passive outflow (no control). Higher flows are a direct result of higher basin water levels under active control.

Because of its control on the LDC and FDC, the on/off setpoint $h_s$ can be used to adapt stormwater basin performance to changes in the stormwater runoff inflow distribution. To demonstrate, the flow rate with an exceedance probability of 5%, $Q_5$, is plotted in Fig. 10 for several

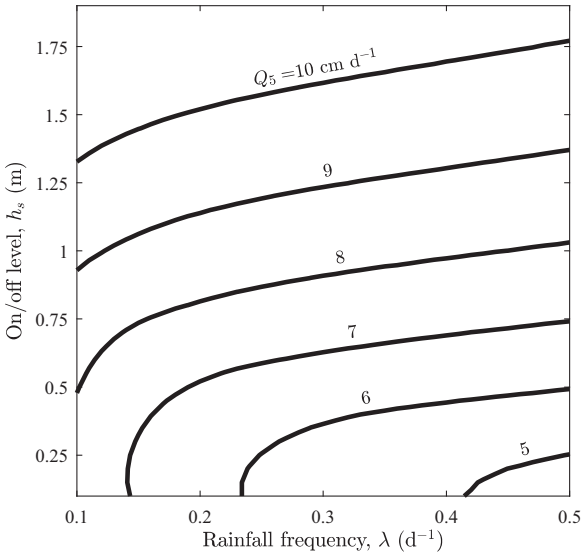


**Fig. 10.** Outflow rate with exceedance probability 5% as a function of the rainfall frequency and the on/off level setpoint. Parameters are the same as in Fig. 3. On the $x$-axis, the total runoff volume is kept constant while the rainfall frequency is varied.

values of the on/off level setpoint and rainfall frequency. Contours of constant $Q_5$ indicate that, for increased rainfall frequency, the on/off level setpoint can be increased to maintain $Q_5$. Therefore, active on/off control can be utilized to enhance resilience of stormwater basins to changing runoff inflow regimes. Similar results can be obtained for other exceedance probabilities.

### 3.5.2. Ensemble average water level and water balance

The steady-state water level PDF can be used to compute the average water balance partitioning to the outflow structure or the emergency overflow and the average basin water level. These quantities represent the average basin function at the seasonal scale. The ensemble average steady-state water balance can be expressed as,

$$\langle Q_i \rangle = \langle Q_s \rangle + \langle Q_o \rangle \tag{17}$$

where the brackets $\langle \cdot \rangle$ denote ensemble averages and subscripts $s$ and $o$ indicate outflow through the structure and emergency overflow, respectively. The ensemble average daily inflow volume is simply, $\langle Q_i \rangle = \alpha \lambda A_s$. The ensemble average overflow volume is related to the frequency of the water level crossing $h_{max}$, $\lambda_o = p_h(h_{max})\rho(h_{max})$ (Porporato et al., 2001). Because the inflow events are exponentially distributed, the overflow volumes are also exponentially distributed with mean $\alpha$ (Bartlett et al., 2015, Eq. 3.21). Therefore, $\langle Q_o \rangle = \alpha p_h(h_{max})\rho(h_{max})A_s$ and $\langle Q_s \rangle = \langle Q_i \rangle - \langle Q_o \rangle$. Finally, the ensemble average water level can be obtained from the PDF by definition, $h = \int_0^{h_{max}} h p_h(h) dh$.

The passive orifice outflow is used as an example. The average fraction of inflow controlled through the outflow structure is,

$$\frac{\langle Q_s \rangle}{\langle Q_i \rangle} = 1 - P_0 \sqrt{h_{max}} \exp\left( -\frac{h_{max}}{\alpha} + \frac{\lambda}{k} \sqrt{h_{max}} \right) \tag{18}$$

where $P_0$ is given in Table 2. The ensemble average water level for a passive orifice outflow can be computed analytically, but is not reported here for brevity. Similar expressions can be obtained for other outflow stage-discharge curves and actively controlled outflows.

Examples of the ensemble average water balance partitioning and the ensemble average water level are illustrated in Fig. 11. Active control increases both the average water level and the runoff volume lost to emergency overflow. Increases in average water level due to active control are not sensitive to rainfall frequency and increase as the on/off setpoint is increased. Increases in emergency overflow due to active control increase with the on/off setpoint and decrease with rainfall frequency.

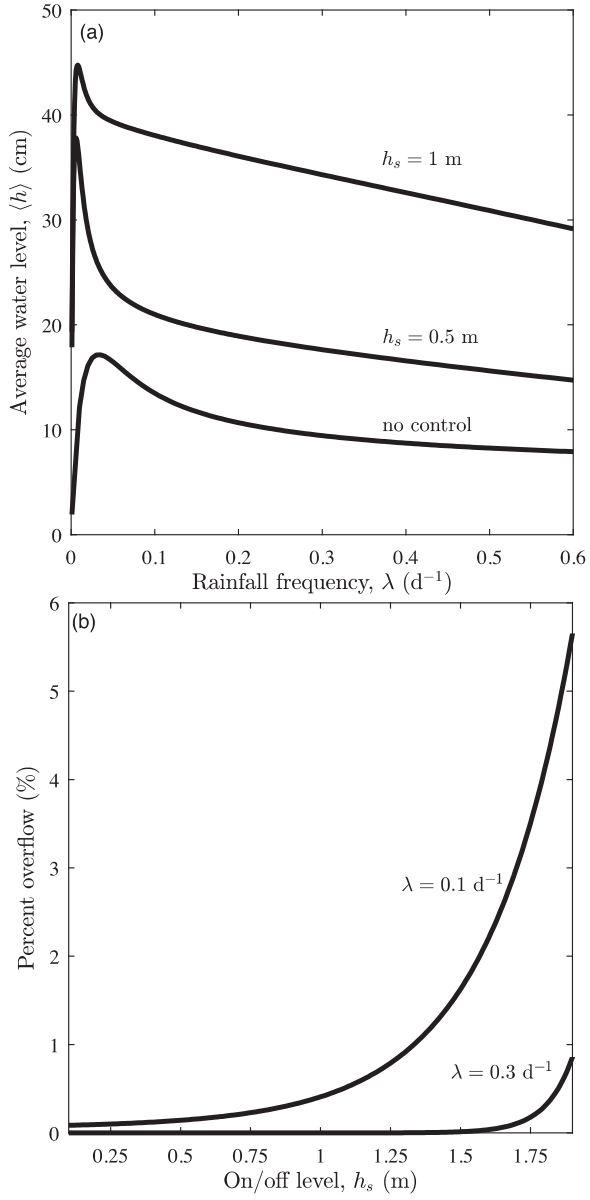


**Fig. 11.** Ensemble average (a) water level and (b) overflow volume as a function of rainfall frequency and on/off setpoint. Parameters are the same as Fig. 3a. On the *x*-axis of (a), the total runoff volume is kept constant while the rainfall frequency is varied.

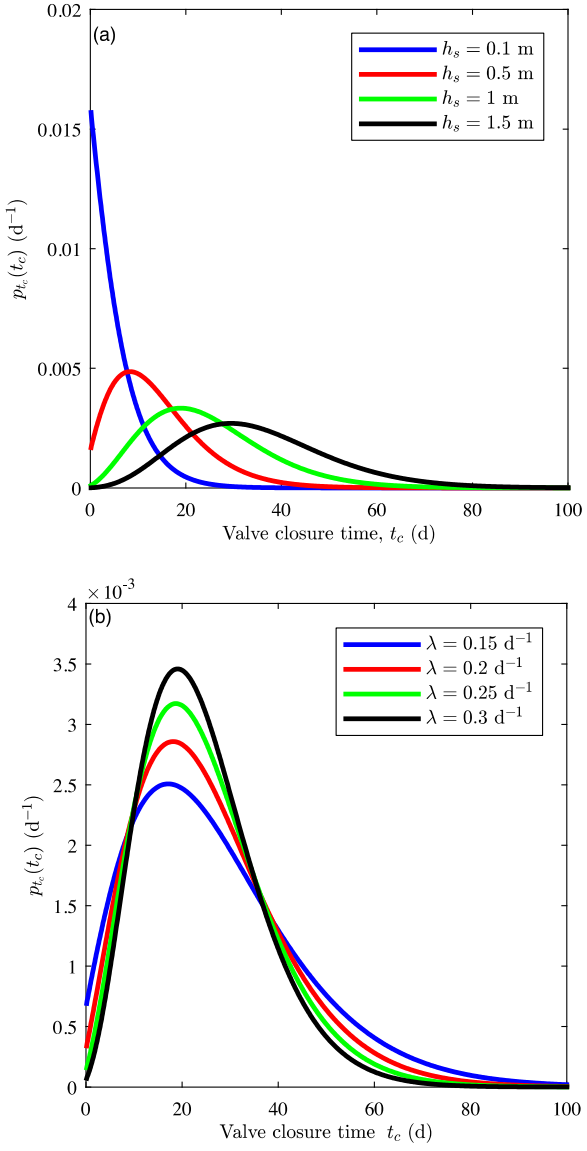


**Fig. 12.** Sensitivity of the valve closure time PDF to (a) $h_s$ and (b) $\lambda$. Other parameters are the same as Fig. 3a. In (b), the total runoff volume is kept constant while the rainfall frequency is varied, i.e., $\langle Q_i \rangle = \lambda\alpha$.

In this example, for on/off setpoints less than about half of the emergency overflow level, the increase in overflow is negligible. Therefore, this simple on/off control rule for active control increases basin storage without significantly increasing overflow.

### 3.5.3. Distribution of the valve closure time

One objective of active, real-time control of stormwater basin outflows is to increase water detention time for enhanced pollutant removal. In addition to the detention time, pollutant removal efficiency also depends on the basin water level. The water level impacts the pollutant concentration through dilution as well as the critical settling velocity (Takamatsu, 2010). On the other hand, increased detention time may have negative consequences such as development of anoxic conditions or pests. The framework introduced here can be used to provide insight into the impact of active controls on pollutant removal through the joint distribution of detention time and water level.

The distribution of times the basin spends in the filling regime (regime 1) and, therefore, the times the valve is closed, can be obtained from the time-dependent solution of the PDF, $p_{h_1}(h,t)$. The filling regime is a compound Poisson process and the PDF of cumulative basin inflows at time $t$ following valve closure is (Daly and Porporato, 2006),

$$p_{h_1}(h,t) = \exp\left(-\frac{h}{\alpha} - \lambda t\right)\left[\sqrt{\frac{\lambda t}{\alpha h}} I_1\left(2\sqrt{\frac{\lambda h t}{\alpha}}\right) + \delta(h)\right] \tag{19}$$

where $I_1(\cdot)$ is the modified Bessel function of the first kind of order 1 (Abramowitz and Stegun, 1972).

The PDF of Eq. (19) can be integrated to define the probability that the valve reopens before a given time, $t$, which is equivalent to the probability that $h(t)$ exceeds $h_s$,

$$P(t_c \le t) = \int_{h_s}^{\infty} p_{h_1}(h,t)\,dh \tag{20}$$

where $t_c$ is a random variable that defines the time between valve closing and opening. Therefore, the PDF of valve closure times is,

$$p_{t_c}(t_c) = \frac{dP(t_c \le t)}{dt} = \frac{d}{dt}\int_{h_s}^{\infty} p_{h_1}(h,t)\,dh. \tag{21}$$

Eq. (21) does not have a closed-form solution. The sensitivity of $p_{t_c}(t_c)$ to $h_s$ and $\lambda$ is illustrated in Fig. 12. As expected, higher $h_s$ leads to

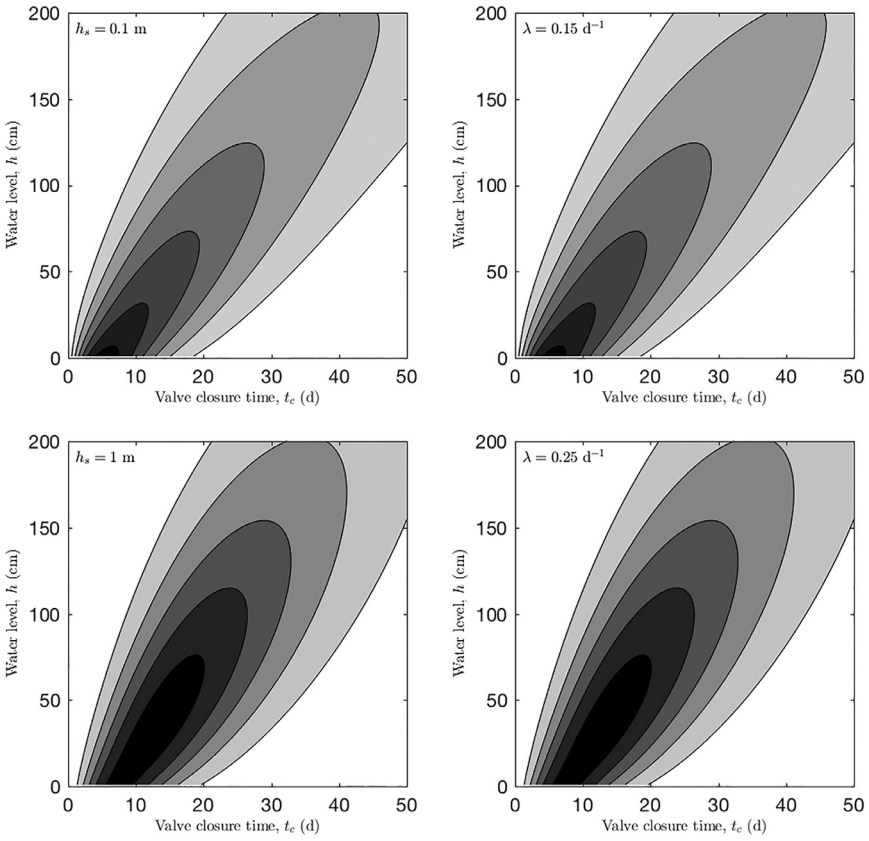


**Fig. 13.** Sensitivity of the joint PDF of the valve closure time and basin water level to (left) $h_s$ and (right) $\lambda$. Other parameters are the same as Fig. 3a. In the right panels, the total runoff volume is kept constant while the rainfall frequency is varied.

longer valve closure times and, therefore, longer detention times. Runoff inflow distributions with more frequent and less intense inflows reduce the variability of the valve closure time, whereas storm frequency has a minor impact on the mode of $p_{t_c}(t_c)$.

Note that Eq. (19) can also be used to define the PDF of $h$ conditional on $t_c$,

$$p_{h|t_c}(h|t_c) = N \exp\left(-\frac{h}{\alpha} - \lambda t_c\right)\left[\sqrt{\frac{\lambda t_c}{\alpha h}} I_1\left(2\sqrt{\frac{\lambda h t_c}{\alpha}}\right) + \delta(h)\right] \tag{22}$$

where $N$ is a normalization constant that accounts for the fact that $h$ is restricted between 0 and $h_s$ in regime 1. The joint distribution of $h$ and $t_c$ can then be obtained combining Eqs. (21) and (22),

$$p_{h,t_c}(h, t_c) = p_{h|t_c}(h|t_c) p_{t_c}(t_c). \tag{23}$$

The sensitivity of $p_{h,t_c}(h, t_c)$ to $h_s$ and $\lambda$ is illustrated in Fig. 13. In general, there is a nearly linear relationship between the modes of the marginal valve closure time and water level distributions. That is, the valve closure time is strongly and positively related to the basin water level. These basin performance metrics have opposite impacts on basin pollutant removal. Assuming settling as the primary pollutant removal process, increased water level increases particle settling time, whereas increased detention time increases the fraction of particles removed from the water column. From this purely hydrologic perspective, it is not clear how important this trade-off is toward an effective balance between water storage and pollutant removal.

## 4. Discussion and conclusions

A stochastic water balance model was developed for stormwater control basins and the model considers both passive and actively controlled outflows. The proposed model joins a number of recent models and experiments aimed at quantifying the variability of urban stormwater infrastructure performance (Daly et al., 2012, 2014; Li et al., 2016). While previous studies have focused on dynamics and performance of bioretention and treatment facilities, the present work addresses stormwater retention and detention basins as well as active real-time control of basin outflows (Kerkez et al., 2016; Mullapudi et al., 2017). The model describes the dynamics of the basin water level $h$ and, given the statistics of the runoff inflow process, provides a probabilistic characterization of the basin hydrologic function. Results include the water level PDF, the joint distribution of valve closure time and water level, and average water balance under different land use, climate, and design characteristics. The water level PDF, which can also be expressed as a level duration curve, leads directly to an analytical expression for the basin flow duration curve. Thus, a full probabilistic description of hydrologic performance in passive and actively controlled stormwater basins has been achieved.

The model presented here has a number of limitations to be addressed in future work. The model assumes the stormwater basin is rectangular and has a constant surface area with depth. This assumption applies to rain barrels and subsurface rainwater harvesting tanks, but most stormwater detention and retention ponds have sloped sides. Secondly, the model assumes a Poisson arrival process for stormwater runoff events and that runoff depths are exponentially distributed. This assumption was shown to apply in the present case study, however, it may not be appropriate in all cases. Finally, the model verification was limited by data availability. During the three months of recorded water level data, there were only 12 storms to estimate the parameters $\alpha$ and $\lambda$. Therefore, confidence in these parameters is low. In addition, the outflow stage-discharge relation parameters were estimated from the data, limiting applicability of Eq. (8) to other ungauged sites.

Analysis of the results demonstrates the role of active outflow control in altering the hydrologic dynamics of stormwater basins. Active control, as defined here, increases water storage volume and detention time, which mitigate increased peak runoff flows and pollutant runoff due to urbanization, respectively. Further, the results show that active outflow control can be employed as an effective practice to adapt stormwater basin outflows to land use or climate changes that alter the timing and frequency of stormwater runoff events. However, active outflow control may increase the likelihood of emergency overflow and reduce the efficiency of pollutant removal by increasing particle settling time. These trade-offs and their implications must be addressed in future work.

This model represents a first step toward understanding the interaction between runoff variability and smart stormwater systems (Mullapudi et al., 2017). As such, our work focuses on the hydrologic performance of single stormwater management facility. The modeling framework can be adapted to investigate progressively more complex systems, including coupled hydrologic and biogeochemical processes and networks of multiple interacting controls.

## Acknowledgments

The authors thank Branko Kerkez and open-storm.org for providing the Ann Arbor basin water level data. AJP and SP acknowledge support from the National Science Foundation Industry/University Cooperative Research Center on Water Equipment & Policy located at the University of Wisconsin Milwaukee (IIP-1540032) and Marquette University (IIP-1540010). MSB acknowledges support through the National Science Foundation through grants EAR-1331846, FESD-1338694, EAR-1316258, and the Duke WISeNet Grant DGE-1068871 and from the AFRI Postdoctoral Fellowship Program Grant No. 2017-67012-26106/Project Accession Number 1011029 from the USDA National Institute of Food and Agriculture. Data and computer code can be obtained by contacting the corresponding author.

## Appendix A. Steady-state water level PDF for the emptying regime

During the emptying regime, the outflow valve is open. Therefore, the water level increases due to stochastic stormwater runoff inflows and decreases due to outflow according to the deterministic stage-discharge relation. At steady-state, the rates at which water level trajectories downcross and upcross a given level $h$ must be equal, i.e.,

$$J^{\downarrow}(h) = J^{\uparrow}(h). \tag{A1}$$

Here, we use this downcrossing and upcrossing rate approach to develop the master equation, based on the cumulative distribution function (CDF), and then solve for the probability density function (PDF) of water level when the valve is open, $p_{h_2}(h)$.

Water level trajectories downcross a level $h$ due to the deterministic outflow $\rho(h)$ and the downcrossing rate is given by (Laio et al., 2001; Brill, 2008),

$$J^{\downarrow}(h) = \rho(h)p_{h_2}(h). \tag{A2}$$

Water trajectories upcross a level $h$ due to both the filling regime (when the valve is closed) and the stochastic jumps of stormwater runoff inflows (when the valve is open), i.e.,

$$J^{\uparrow}(h) = C_U + \lambda \int_{u=h_{min}}^{h} \exp\left[-\frac{h-u}{\alpha}\right] p_{h_2}(u)du \tag{A3}$$

where $C_U$ is the average upcrossing rate at which the filling regime enters the emptying regime (i.e., the average rate at which $h_s$ is crossed and the outflow structure opens) and the second term on the RHS is the upcrossing rate due to runoff inflow (Laio et al., 2001). Thus, following Eq. (A1), the steady-state master equation is given as,

$$\rho(h)p_{h_2}(h) = C_U + \lambda \int_{u=h_{min}}^{h} \exp\left[-\frac{h-u}{\alpha}\right] p_{h_2}(u)du. \tag{A4}$$

where the LHS represents the downcrossing rate and the RHS represents the upcrossing rate.

Multiplying Eq. (A4) by $\exp(\frac{h}{\alpha})$ and differentiating with respect to $h$ yields (Cox and Isham, 1986; Rodriguez-Iturbe et al., 1999),

$$\frac{d}{dh}\left[\rho(h)p_{h_2}(h)\right] + \rho(h)p_{h_2}(h)\left[\frac{1}{\alpha} - \frac{\lambda}{\rho(h)}\right] = \frac{C_U}{\alpha}. \tag{A5}$$

In Eq. (A5), the PDF $p_{h_2}(h)$ consists of two distinct parts,

$$p_{h_2}(h) = \tilde{p}_{h_2}(h) + \hat{p}_{h_2}(h) \tag{A6}$$

where $\tilde{p}_{h_2}(h)$ is valid for $h_{min} < h \le h_s$ when $C_U \neq 0$ and $\hat{p}_{h_2}(h)$ is valid for $h_s < h < \infty$ when $C_U = 0$. For the first case, Eq. (A5) can be integrated to obtain the steady-state water level PDF for the emptying regime,

$$\tilde{p}_{h_2}(h) = \frac{C_U}{\rho(h)} \exp[-F(h)]\left\{1 + \frac{1}{\alpha}\int_{u=h_{min}}^{h} \exp[F(u)]du\right\} \tag{A7}$$

where $F(u) = \int_0^u (\frac{1}{\alpha} - \frac{\lambda}{\rho(y)})dy$ and $C_U$ is the normalization constant of the PDF such that $\int_{h_{min}}^{h_{max}} \tilde{p}_{h_2}(h)dh = 1$ (Vico and Porporato, 2011). For the second case, when $C_U = 0$, the solution to Eq. (A5) is (Botter et al., 2009),

$$\hat{p}_{h_2}(h) = \frac{C}{\rho(h)} \exp[-F(h)]. \tag{A8}$$

The solutions (A7) and (A8) must be continuous at $h_s$, i.e., $\tilde{p}_{h_2}(h_s) = \hat{p}_{h_2}(h_s)$. Therefore, $C = C_U\{1 + \frac{1}{\alpha}\int_{u=h_{min}}^{h_s} \exp[F(u)]du\}$ and we can compactly write the complete solution of Eq. (A6),

$$p_{h_2}(h) = \frac{C_U}{\rho(h)} \exp[-F(h)]\left\{1 + \frac{1}{\alpha}\int_{u=h_{min}}^{h_s+(h-h_s)\Theta(h_s-h)} \exp[F(u)]du\right\} \tag{A9}$$

where $\Theta(\cdot)$ is the Heaviside step function. Based on Eq. (A9), the solution for the general stage-discharge relation $\rho(h)$ is,

$$p_{h_2}(h) = \frac{C_U}{kh^b} \exp\left[-\frac{h}{\alpha} - \frac{\lambda}{k(1-b)}h^{1-b}\right] \left\{1 + \frac{1}{\alpha}\int_{h_{min}}^{h_s+(h-h_s)\Theta(h_s-h)} \exp\left[\frac{h}{\alpha} + \frac{\lambda}{k(1-b)}h^{1-b}\right]dh\right\} \tag{A10}$$

which is found from Eq. (A8) by substituting for the general state-discharge relationship of Eq. (4).

## References

Abramowitz, M., Stegun, I.A., 1972. Handbook of mathematical functions with formulas, grpahs and mathematical tables. Natl. Bureau Stand. Appl. Math. Ser. 300.
Bartlett, M.S., Daly, E., McDonnell, J.J., Parolari, A.J., Porporato, A., 2015. Stochastic rainfall-runoff model with explicit soil moisture dynamics, 471.
Bartlett, M.S., Parolari, A.J., McDonnell, J.J., Porporato, A., 2016a. Beyond the SCS-CN method: a theoretical framework for spatially lumped rainfall-runoff response. Water Resour. Res. 52.
Bartlett, M.S., Parolari, A.J., McDonnell, J.J., Porporato, A., 2016b. Framework for event-based semidistributed modeling that unifies the SCS-CN method, VIC, PDM, and TOPMODEL. Water Resour. Res. 52.
Bhaskar, A.S., Beesley, L., Burns, M.J., Fletcher, T.D., Hamel, P., Oldham, C.E., Roy, A.H., 2016. Will it rise or will it fall? Managing the complex effects of urbanization on base flow. Freshwater Sci. 35, 293–310.
Botter, G., Porporato, A., Rodriguez-Iturbe, I., Rinaldo, A., 2009. Nonlinear storage-discharge relations and catchment streamflow regimes. Water Resour. Res..
Brill, P.H., 2008. In: Hillier, F.S. (Ed.), Level Crossing Methods in Stochastic Models. Springer.
Chen, J., Adams, B.J., 2007. Development of analytical models for estimation of urban stormwater runoff. J. Hydrol. 336, 458–469.
Cox, D.R., Isham, V., 1986. The virtual waiting-time and related processes. Adv. Appl. Probab..
Daly, E., Bach, P.M., Deletic, A., 2014. Stormwater pollutant runoff: a stochastic approach. Adv. Water Resour..
Daly, E., Deletic, A., Hatt, B.E., Fletcher, T.D., 2012. Modelling of stormwater biofilters under random hydrologic variability: a case study of a car park at Monash University, Victoria (Australia). Hydrol. Processes 26, 3416–3424.
Daly, E., Porporato, A., 2006. Impact of hydroclimatic fluctuations on the soil water balance. Water Resour. Res..

Gaborit, E., Muschalla, D., Vallet, B., Vanrolleghem, P.A., Anctil, F., 2013. Improving the performance of stormwater detention basins by real-time control using rainfall forecasts. Urban Water J. 10, 230–246.
Guo, Y., 2016. Stochastic analysis of hydrologic operation of green roofs. J. Hydrol. Eng. 21, 04016016.
Jacopin, C., Lucas, E., Desbordes, M., Bourgogne, P., 2001. Optimisation of operational management practices for the detention basins. Water Sci. Technol. 277–285.
Kerkez, B., Gruden, C., Lewis, M., Montestruque, L., Quigley, M., Wong, B., Bedig, A., Kertesz, R., Braun, T., Cadwalader, O., et al., 2016. Smarter stormwater systems. Environ. Sci. Technol. 50, 7267–7273.
Kunkel, K.E., Karl, T.R., Brooks, H., Kossin, J., Lawrimore, J.H., Arndt, D., Bosart, L., Changnon, D., Cutter, S.L., Doesken, N., et al., 2013. Monitoring and understanding trends in extreme storms: state of knowledge. Bull. Am. Meteorol. Soc. 94, 499–514.
Laio, F., Porporato, A., Fernandez-Illescas, C., Rodriguez-Iturbe, I., 2001. Plants in water-controlled ecosystems: active role in hydrologic processes and response to water stress II. Probabilistic soil moisture dynamics. Adv. Water Resour. 24, 745–762.
Leopold, L., 1968. In: Hydrology for Urban Land Planning - A Guidebook on the Hydrologic Effects of Urban Land Use, 554. Geological Survey Circular, pp. 1–21.
Li, Y., McCarthy, D.T., Deletic, A., 2016. Escherichia coli removal in copper-zeolite-integrated stormwater biofilters: effect of vegetation, operational time, intermittent drying weather. Ecol. Eng. 90, 234–243.
Loganathan, G.V., Delleur, J.W., 1984. Effects of urbanization on frequencies of overflows and pollutant loadings from storm sewer overflows: a derived distribution approach. Water Resour. Res. 20, 857–865.
Mejía, A., Daly, E., Rossel, F., Jovanovic, T., Gironás, J., 2014. A stochastic model of streamflow for urbanized basins. Water Resour. Res. 50, 1984–2001.
Mullapudi, A., Wong, B.P., Kerkez, B., 2017. Emerging investigators series: building a theory for smart stormwater systems. Environ. Sci. 3, 66–77.
Muschalla, D., Vallet, B., Anctil, F., Lessard, P., Pelletier, G., Vanrolleghem, P.A., 2014. Ecohydraulic-driven real-time control of stormwater basins. J. Hydrol. 511, 82–91.
NRCS. 1986. Urban Hydrology for Small Watersheds TR-55. USDA Natural Resource Conservation Service Conservation Engeneering Division Technical Release 55: 164.
Porporato, A., Laio, F., Ridolfi, L., Rodriguez-Iturbe, I., 2001. Plants in water-controlled ecosystems: active role in hydrologic processes and response to water stress III. Vegetation water stress. Adv. Water Resour. 24, 725–744.
Porporato, A., Vico, G., Fay, P.A., 2006. Superstatistics of hydro-climatic fluctuations and interannual ecosystem productivity. Geophys. Res. Lett. 33.
Rodriguez-Iturbe, I., Porporato, A., Ridolfi, L., Isham, V., Coxi, D.R., 1999. Probabilistic modelling of water balance at a point: the role of climate, soil and vegetation. Proc. R. Soc. A 455, 3789–3805.
Takamatsu, M., 2010. Hydraulic model for sedimentation in storm-water detention basins. J. Environ. Eng..
Vico, G., Porporato, A., 2011. From rainfed agriculture to stress-avoidance irrigation: I. A generalized irrigation scheme with stochastic soil moisture. Adv. Water Resour..
Wisconsin Department of Natural Resources, 2007. Wet Detention Pond Conservation Practice Standard.
Yang, L., Smith, J.A., Wright, D.B., Baeck, M.L., Villarini, G., Tian, F., Hu, H., 2013. Urbanization and climate change: an examination of nonstationarities in urban flooding. J. Hydrometeorol. 14, 1791–1809.